



Brittle tectonic structures and palaeostress analysis in the Isle of Wight, Wessex basin, southern U.K.

S. Vandycke^{a,*}, F. Bergerat^b

^aLaboratoire de Géologie Fondamentale et Appliquée, Faculté Polytechnique de Mons, 9 rue de Houdain, 7000 Mons, Belgium

^bLaboratoire de Tectonique, ESA 7072 CNRS-UPMC, Bte 129, 4 place Jussieu, 75252 Paris cedex 05, France

Received 31 January 2000; accepted 17 July 2000

Abstract

Brittle tectonic analysis of Cretaceous–Paleogene sediments at a total of 17 sites located in the Isle of Wight (U.K.) enables four main tectonic events that occurred prior to and after the folding to be identified and successive palaeostress tensors to be determined using the inversion method. Three of the events can be shown to have occurred prior to the folding: (1) a syn-sedimentary extension of Upper Cretaceous age; (2) a strike-slip faulting regime with an ESE–WNW direction of compression; (3) a compressional regime, marked by strike-slip faulting, with an NNE–SSW to N–S direction of compression. The fourth and last compressional event took place after the folding and is characterised both by reverse and strike-slip faulting, with a dominant N–S direction of compression. Syn-folding faults also developed between the third and fourth events. All four events can be connected to the extensional tectonics and different steps of structural inversion, both of which were integral to the development and evolution of the Wessex basin. © 2001 Elsevier Science Ltd. All rights reserved.

1. Introduction

This paper describes the results of a brittle tectonic analysis carried out in the Isle of Wight, a classical location for study of inversion structures of the Wessex basin, southern England (Fig. 1). Despite being the focus of many studies, few fault slip data have been analysed in the Purbeck–Isle of Wight area to date. Even those few studies that have been undertaken on the Dorset coast (e.g. Bevan, 1985; Ameen, 1990) and in the Isle of Wight (e.g. Bevan, 1984) did not use fault slip data inversion methods. Such an analysis, in terms of stress tensor reconstruction, can help in the understanding of tectonic processes involved in the creation and evolution of structures. The purpose of this work is to describe and interpret the different mesofault systems that affected the Isle of Wight before and after the inversion process in terms of palaeostress tensors. The results allow the meso-scale faulting seen in the area to be constrained in relation to large-scale folding and basin inversion, thereby improving structural understanding of the region and highlighting the regional geodynamics.

2. Geological setting

The Isle of Wight is located between the Weald and Channel basins (Fig. 1), both part of the composite Wessex basin, named and recognised as a major depocentre by Kent (1949). The structure and evolution of the Wessex basin has recently been outlined, with the increased exploration interest, from geophysical and borehole data acquisition (e.g. Lake and Karner, 1987; Stoneley, 1982; Underhill and Stoneley, 1998), and also with a field-based approach (e.g. Jenkyns and Senior, 1991).

Because of the exceptional coastal exposures, the stratigraphy of the exposed Cretaceous–Tertiary series of the Isle of Wight is well known. Stratigraphic syntheses have been carried out during the last decade (e.g. Hamblin et al., 1992; Ainsworth et al., 1998a,b; Cole and Harding, 1998) and this section. We use herein the regional names of Formations and Members as defined in Hamblin et al. (1992). A summarised and simplified description of the outcropping succession is provided in Fig. 2.

From a structural point of view, during the last decade, the integration of well data with the seismic data have given new insights into the deep structures of the Wessex basin in general, and the Isle of Wight in particular (e.g. Chadwick, 1993; Butler, 1998; Hawkes et al., 1998; Underhill and Paterson, 1998; Underhill and Stoneley, 1998). The tectonic evolution of the Weald and Channel basins can

* Corresponding author. Fax: +32-65-374-610.

E-mail addresses: sara.vandycke@fpms.ac.be (S. Vandycke), bergerat@lgs.jussieu.fr (F. Bergerat).

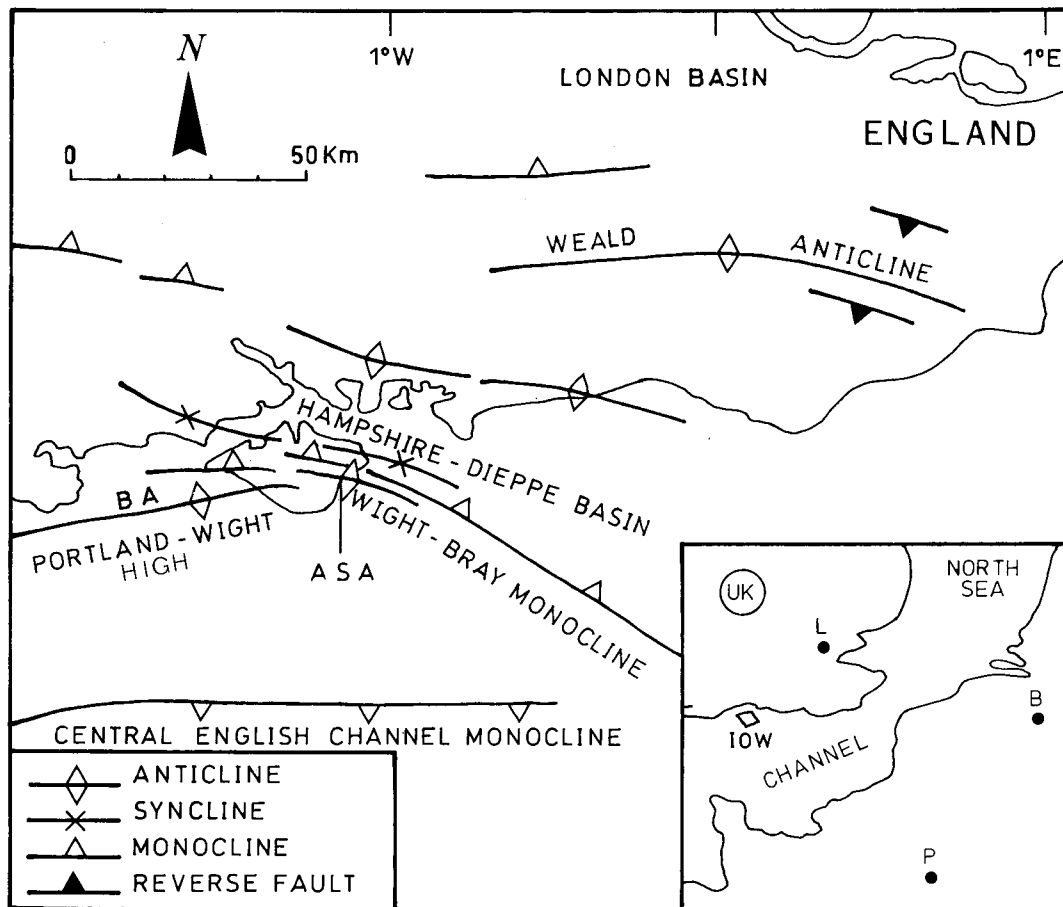


Fig. 1. Location map of the Isle of Wight (IOW in the inset), showing the main Tertiary structural elements (modified from Hamblin et al., 1992). ASA, Arreton–Sandown anticline; BA, Brighstone anticline. Inset: B, Brussels; L, London; P, Paris; IOW, Isle of Wight.

be split into three main phases: (1) a rift-subsidence process from the Late Jurassic to Mid-Cretaceous; (2) a subsequent Late Cretaceous thermal subsidence; and (3) inversion movements on the pre-existing normal faults leading to the development of hanging wall anticlines. The geometry of the major extensional structures (which are not visible at the surface) can be seen in seismic profiles and reconstructed cross-sections recently published by Butler (1998), Hawkes et al. (1998), and Underhill and Paterson (1998). The corresponding outcropping structures in the Isle of Wight are the E–W-trending “en échelon” Brighstone and Arreton–Sandown inversion anticlines, marked on their northern flank by north-facing flexures (Fig. 1).

As emphasised by Underhill and Paterson (1998), despite recent advances in understanding of the inversion process, several aspects of their development and evolution remain unresolved, for example the spatial distribution of related macro- and meso-scale structures. Only the study of well-exposed inverted basins with available subsurface data can help to highlight this process. The continuity of the coastal exposures in the Cretaceous to Paleogene Formations on the Isle of Wight, combined with the horizontal to near-vertical bedding, allow us to characterise the brittle deformation in

space and time and to integrate its evolution in the tectonic inversion history of the Wessex basin.

3. Methodology

All the outcropping stratigraphical levels were visited, but only the Upper Chalk Formation and the Priabonian Bembridge Beds provide enough data to be analysed for stress tensor reconstruction. Therefore, brittle tectonic analysis has been carried out in these stratigraphical levels at a total of 17 sites located along the cliffs and road cuts, as well as in several quarries, in the middle of Isle of Wight (see Figs. 2, 9 and 10). The mesofractures measured are tension gashes, joints and striated fault planes. About 30–150 fault planes bearing slickenslide lineations have been collected in each site. Most of the measured faults present a small displacement (centimetric to metric); some of them have been filled by flint or by sandy-clay sediments.

3.1. Computing palaeostress tensors

The inversion methods used here for fault slip data analysis have been described in detail by Angelier (1984, 1990, 1994) and applied successfully in the western European

TERTIARY	OLIGOCENE	30	Chatian				
			Rupelian	Grey and green muds	Hamstead Beds (96 m)	17	
	EOCENE	36	Priabonian	Marly limestones (1-19 m) Muds, silts, sands, marls, limestones (75-100 m)	Bembridge Beds	3, 16	
		39	Bartonian	Silts, sands	Headon Beds		
		42			Barton Beds (185 m)		
		49	Lutetian	Sandy clays, sandy limestones	Brackesham Beds	15	
		54	Ypresian	Sands, calcareous sandstones (63-83 m) Clays, silts	London clay F ^{10m} (60-160 m)	14	
		60	Thanetian	Fluvio-marine mottled clays	Reading F ^{10m} (40 m)		
	PALEOCENE	65	Danian				
			Maastrichtian				
	CRETACEOUS	UPPER	74	Campanian			
			84	Santonian	White Chalk	Upper Chalk (400 m)	1, 2 4, 5, 6 7, 8, 9
			88	Coniacian			
			89			Middle Chalk (40 m)	
		92	Turonian	White Chalk			
		96	Cenomanian	Plenus Marls (3 m) Chalk Marl, Grey Chalk Glaucous Marls (3 m)	Lower Chalk (60 m)	10 11	
		LOWER	Albian	Sandy clays, sandstones Clays, mudstones, silstones	Upper Greensand (40 m) Gault Clay (0-12 m)		

Fig. 2. Cretaceous and Tertiary stratigraphy of the Hampshire Basin–Isle of Wight (simplified from Hamblin et al., 1992). From left to right: system, standard stage and age, lithological description, lithostratigraphic formations and thicknesses, site numbers. 1. Freswater Bay; 2. Compton Bay; 3. The Quarries; 4. Shalcombe; 5. Brighstone; 6. Shorwell; 7. Garstons; 8. Newport; 9. Arretton; 10. Niton; 11. Ventnor; 12. Culvercliff 1; 13. Culvercliff 2; 14. Whitecliff Bay 1; 15. Whitecliff Bay 2; 16. Bembridge; 17. Yarmouth.

platform by Bergerat (1985, 1987). Several studies have been conducted in other Cretaceous areas in NW Europe displaying inferred palaeostress reconstructions (Dorset and Wight in U.K.: Bevan, 1984, 1985; southwestern U.K., Boulonnais, Normandie in northwestern France: Bevan and Hancock, 1986) or computed palaeostress reconstructions (Boulonnais in western France: Vandycke and Bergerat, 1992; Kent in U.K.: Bergerat and Vandycke, 1994; Mons Basin in Belgium: Vandycke and Bergerat 1989, Vandycke et al. 1991; Champagne in eastern France: Coulon, 1992). The inversion method that has been used herein (*INVDIR* program; see Angelier, 1990) consists of determining the best-fitting reduced palaeostress tensor for a given fault slip data set, thus identifying the attitude of the three principal stress axes (maximum, intermediate and minimum stress: σ_1 , σ_2 and σ_3 , respectively), and the ratio

$\Phi = (\sigma_2 - \sigma_3)/(\sigma_1 - \sigma_3)$ of principal stress magnitudes. Determination of stress axes is strengthened by the analysis of the other brittle structures, such as tension gashes and joints, that can represent extensive, hybrid or shear fractures, according to Hancock's classification (1985).

All the aforementioned studies were carried out in areas that are weakly affected by tectonism. In these regions, the palaeostress succession has been easily established because the measurements were made in subhorizontal bedding and numerous chronological criteria helped to establish at least a relative chronology of deformations. On the contrary, in the Isle of Wight, the bedding is horizontal to moderate- or steep-dipping, especially in the large E–W-trending flexures affecting the area, that make the reconstruction of deformation more difficult to establish. Such polyphase and folded structures have already been described in other

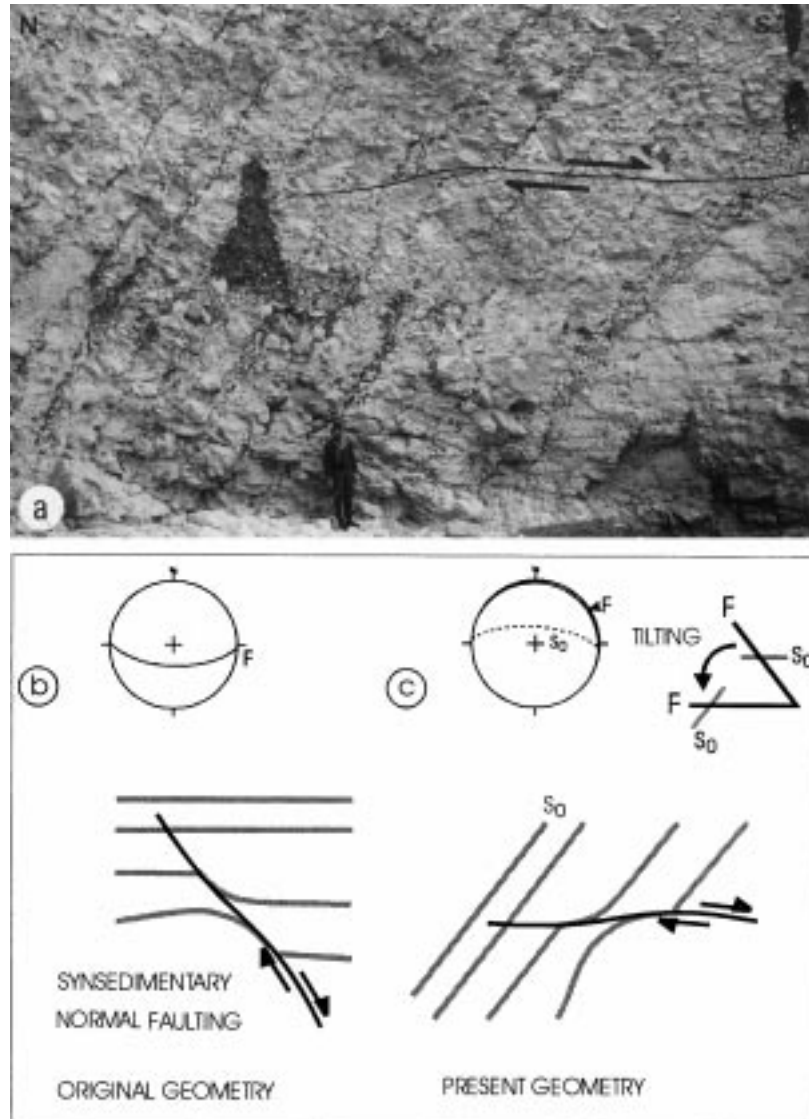


Fig. 3. Example of an apparent flat fault in Upper Chalk at Freshwater Bay (a). Schemes and diagrams of the fault (F) and the bedding (S_0) in their initial position (b) and in their present position (c). This fault is in fact a syn-sedimentary normal fault of Upper Cretaceous age. The tilting occurred during tertiary inversion of the Brighstone anticline (see text for details). Key to stereoplots as for Fig. 6.

tectonic contexts (e.g. Angelier et al., 1986; Bouroz et al., 1989; Reches, 1978, Reches and Johnson, 1978; Hancock, 1985; Turner and Hancock, 1990). These different studies established a precise chronology between the brittle and folding deformations. The same type of analysis, involving these two types of deformations, has been carried out in our study of the Isle of Wight. We paid particular attention to the geometrical relationships between folding and faulting, and therefore to the characterisation of pre-, syn- and post-folding tectonic events.

The fault population used for this analysis is composed of mesofaults as defined by Bevan (1984), embracing structures that range in size from a few centimetres to a few decametres, that are observable in a single continuous exposure.

3.2. Dating successive events

The principal guide for distinguishing the different fault sets are (1) consideration of the age of the rocks affected by a certain deformation, (2) characterisation of the syn-sedimentary faults, (3) the use of tilted structures, (4) cross-cutting relationships and (5) superimposed striae on the same fault plane. One of the major difficulties has been to find structurally complicated sites, with single tectonic events represented by a uniform fault system that allows the establishment of a base for the separation of the different subsets. We discuss below these different criteria.

Evidence for establishing the chronology of tectonic events is sometimes obtained by considering the age of the rocks affected. For example, in the present study, the

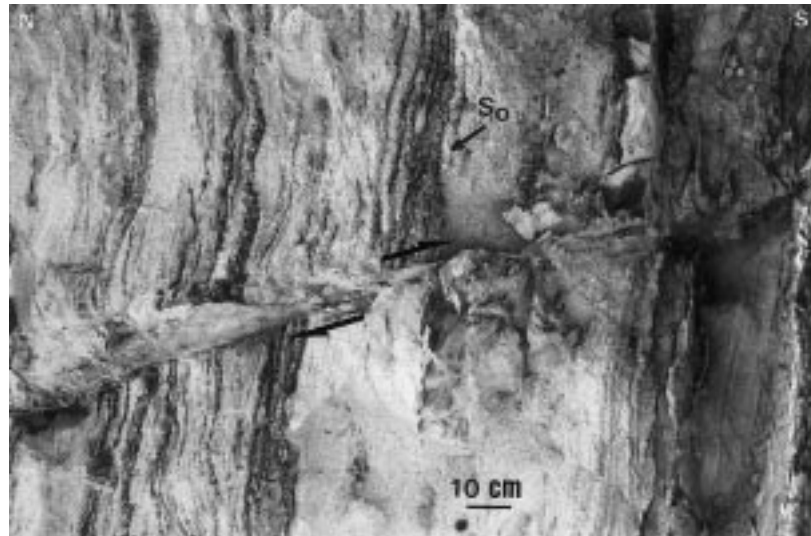


Fig. 4. Example of a reverse fault (azimuth 130° , dip 45°N) in the Bagshot Beds (part of the Brackesham Beds) at Whitecliff Bay (bedding: $105^\circ\text{--}85^\circ\text{N}$). The tilting occurred during tertiary inversion of the Sandown anticline.

Bembridge limestones are only affected by E–W reverse faults and NW–SE and NE–SW conjugate strike-slip faults, both types characterising a roughly N–S compression. This compressional event is thus demonstrably post-Priabonian in age. The other fault sets (see Section 3.3) have never been recognised in the Bembridge limestones and can be considered as pre-Priabonian in age.

Another chronological argument is the presence of syn-sedimentary faulting. An example of a syn-sedimentary tilted normal fault that is subhorizontal with respect to the present datum is shown in Fig. 3. This fault does not cross the uppermost flint levels (strongly dipping to the left on the photograph). Such a geometry dates this as syn-sedimentary faulting of the Upper Cretaceous. The tip of this fault can be interpreted as characteristic of a syn-folding extension fault (Bevan, 1984). However, some other normal faults have been observed in horizontal Cretaceous layers in other sites. These faults cannot be explained by the folding process and, on the other hand, formed prior to the strike-slip and reverse faulting related to the inversion phase. Therefore, it is likely that such normal faults would be, at least in part, syn-sedimentary and thus of Upper Cretaceous age. Note that Nowell (1995) already pointed out the syn-sedimentary growth faults in the Upper Chalk in the Purbeck–Isle of Wight monocline.

It is not always possible to characterise the pre-tilting faulting in the field (e.g. when no syn-sedimentary features are available) but, from the results of the inversion, pre-tilting faulting is implicated where none of the principal stress axes is vertical. When the calculated stresses include two principal stresses contained in the tilted bedding plane, they do not fit with the Anderson (1942) model. In that case, these two principal stresses become horizontal after back-tilting around the bedding plane. These back-tilted stress states are in agreement with the Andersonian

model and the related faulting is thus related to a pre-folding deformation.

An example of geometrical relationships between faulting and folding is given in Fig. 4, which shows a late reverse fault affecting Eocene sub-vertical beds and due to an NNE–SSW compression. In fact, this fault would be a syn-fold normal fault due to layer-parallel extension, as described by Bevan (1984). However, some reverse faults related to the same N–S to NNE–SSW compression can be observed in flat layers of the Bembridge limestones (Table 1), thereby demonstrating the occurrence of post-folding reverse faults.

The geometrical relationships between faults represent another kind of chronological criteria. A cross-cutting relationship between two faults which are reverse with respect to the present datum is shown in Fig. 5. Fault A looks like a steeply dipping reverse fault, but in fact it is a bedding plane bearing bedding-parallel slip. The second fault (B), cutting A, is reverse and formed after the folding. In this case, the first fault (A) is related to the folding process and the second one formed after folding.

The last criterion of relative chronology, and one of the most reliable due to its not being dependent on potentially ambiguous field interpretations, is the fault planes bearing two or more superposed slickenside lineations (striae). For instance, some of the early normal faults bear one set of striae related to their normal motion and a second one either related to a later strike-slip motion or to a later reverse motion. Some strike-slip faults are also found with a second striation corresponding to later normal motion.

3.3. Unravelling polyphase faulting and folding

Most of the sites we analysed display evidence of polyphase faulting and they therefore include different fault

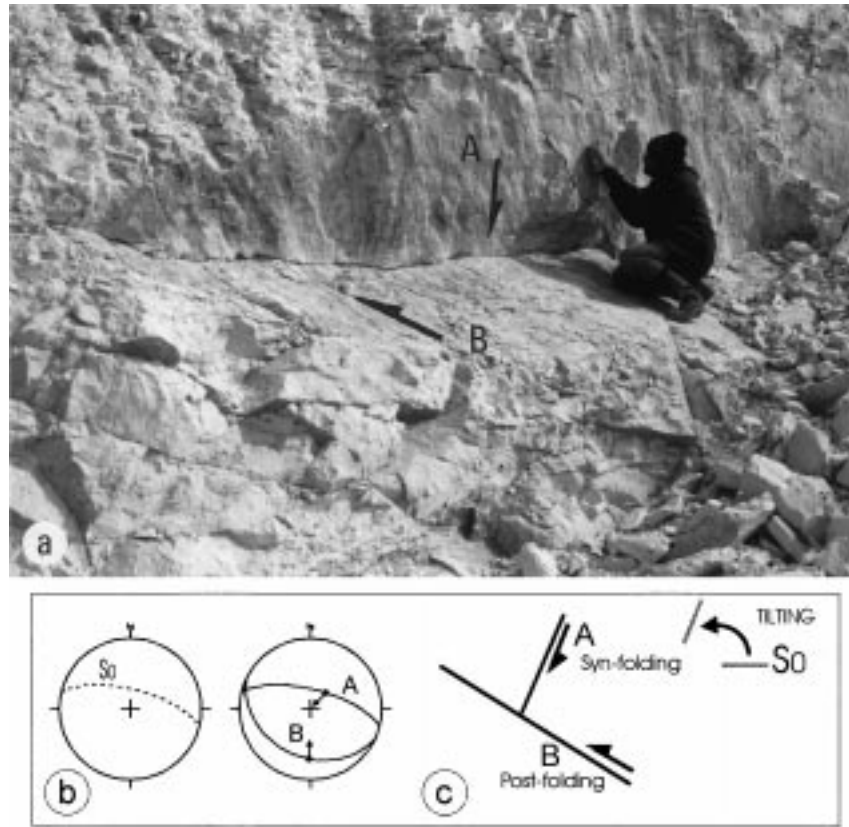


Fig. 5. Example of geometrical relationships between two faults in the Upper Chalk in the Arreton Quarry (a). Fault A (azimuth 115° , dip 65° N) corresponds to a tilted bedding plane bearing bedding parallel slip. Fault B, cutting A, is a post-tilting reverse fault (azimuth 115° , dip 30° S). Diagrams (b) illustrate the bedding plane (S_0) and the two faults (A and B) in their present position. Schemes (c) represent the two faults in their present position and the manner of rotation for fault A (see text for details). Key to stereoplots as for Fig. 6.

Table 1
Palaeostress tensor computations based on fault slip analyses in the Isle of Wight

Site	Lithology	Bedding S_0	Number of faults	Trend and plunge of			RUP (%)	Φ	α ($^\circ$)	Tectonic regime
				σ_1	σ_2	σ_3				
Extensional regime										
9. Arreton	Upper Chalk	120/60N	14	204/80	331/06	062/08	17	0.5	6	E ENE–WSW
13. Culvercliff 2	Upper Chalk	099/65N	21	235/78	131/03	041/12	18	0.4	7	E NE–SW
Strike-slip events before folding, late Cretaceous										
2. Compton Bay	Upper Chalk	090/40N	10	116/07	023/27	219/62	38	0.1	15	X WNW–ESE
2. Compton Bay	Upper Chalk	090/40N	8	042/10	150/60	306/29	41	0.2	12	X NE–SW
5. Brighstone	Upper Chalk	113/45N	4	097/03	333/87	187/04	15	0.4	2	X WNW–ESE
9. Arreton	Upper Chalk	099/65N	8	112/07	213/56	017/33	32	0.3	10	X WNW–ESE
13. Culvercliff 2	Upper Chalk	120/60N	8	112/17	264/71	020/09	41	0.3	12	X WNW–ESE
Strike slip or reverse events during/afterfolding, N–S compression										
1. Freshwater Bay	Upper Chalk	090/69N	11	176/06	085/07	303/81	31	0.1	15	XC N–S
2. Compton Bay	Upper Chalk	090/40N	7	343/17	127/70	249/11	39	0.4	14	X N–S
8. Newport	Upper Chalk	115/67N	16	017/02	284/51	108/39	42	0.3	18	XC N–S
9. Arreton	Upper Chalk	099/65N	15	015/05	284/10	129/79	28	0.6	13	XC N–S
12. Culvercliff 1	Upper Chalk	107/62N	9	007/08	275/16	123/72	20	0.4	9	XC N–S
13. Culvercliff 2	Upper Chalk	120/62N	10	011/21	278/08	169/68	35	0.4	9	C N–S
3. The Quarries	Bembridge Lim.	025/06E	13	358/07	088/00	182/83	42	0.4	10	C N–S
16. Bembridge	Bembridge Lim.	062/05N	9	022/01	112/02	265/88	21	0.5	4	C N–S

RUP and α are quality estimators: average RUP values below 50% and average α values below 25° indicate good fits between computed shear stress and actual fault slip data. E, X and C indicate extensional, strike-slip and compressional regimes, respectively; the direction is that of σ_1 for X and C regimes, and σ_3 for E regimes.

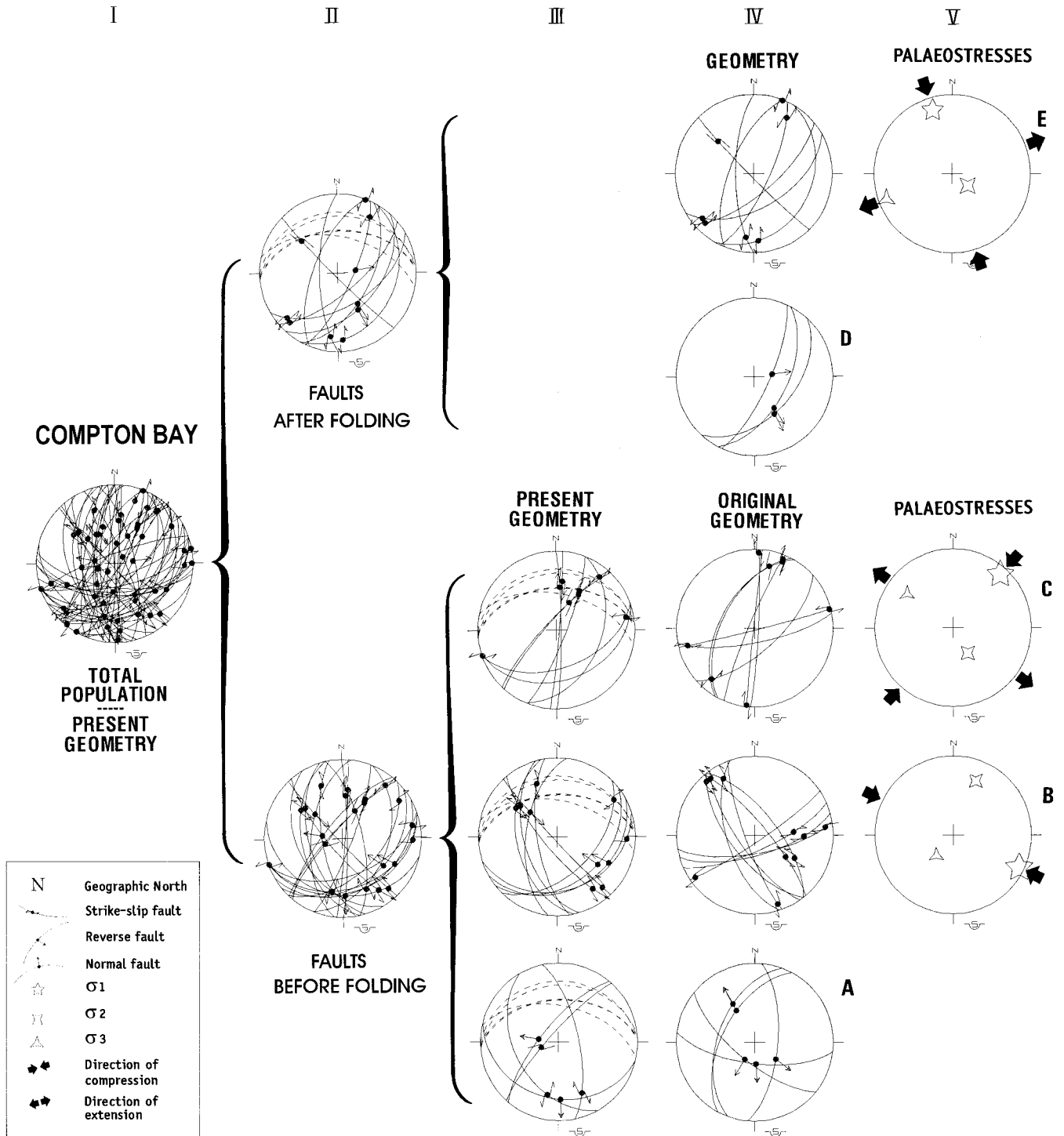


Fig. 6. Geometrical and palaeostress analysis of faulting at Compton Bay. The total population of faults (original setting, Column I) regroups the faults formed before and after flexure. A first analysis allows separation of this population, on the basis of both geometrical and relative chronology criteria, into two sets, including the pre-flexure faults and the post-flexure faults (Column II). The faults that occurred before flexure (present geometry, Column III) are tilted back around the average bedding (rotation of 50–60° around a 90°N–100°E trending axis). Their original geometry is reconstituted (Column IV). Five different fault sets are characterised and the corresponding stress tensors are calculated where the number of faults is sufficient (Column V). All stereoplots are Schmidt’s projection of the lower hemisphere.

subsets. The separation between the different tectonic events has been established with the aid of the sort of chronological criteria discussed above, geometrical relationships and analytical arguments. Only an accurate examination of the

fault attitudes relative to the bedding and a careful sorting based on mechanical consistencies permit discrimination of a valid pattern of successive tectonic events.

Examples of two characteristic analyses are shown in Fig. 6

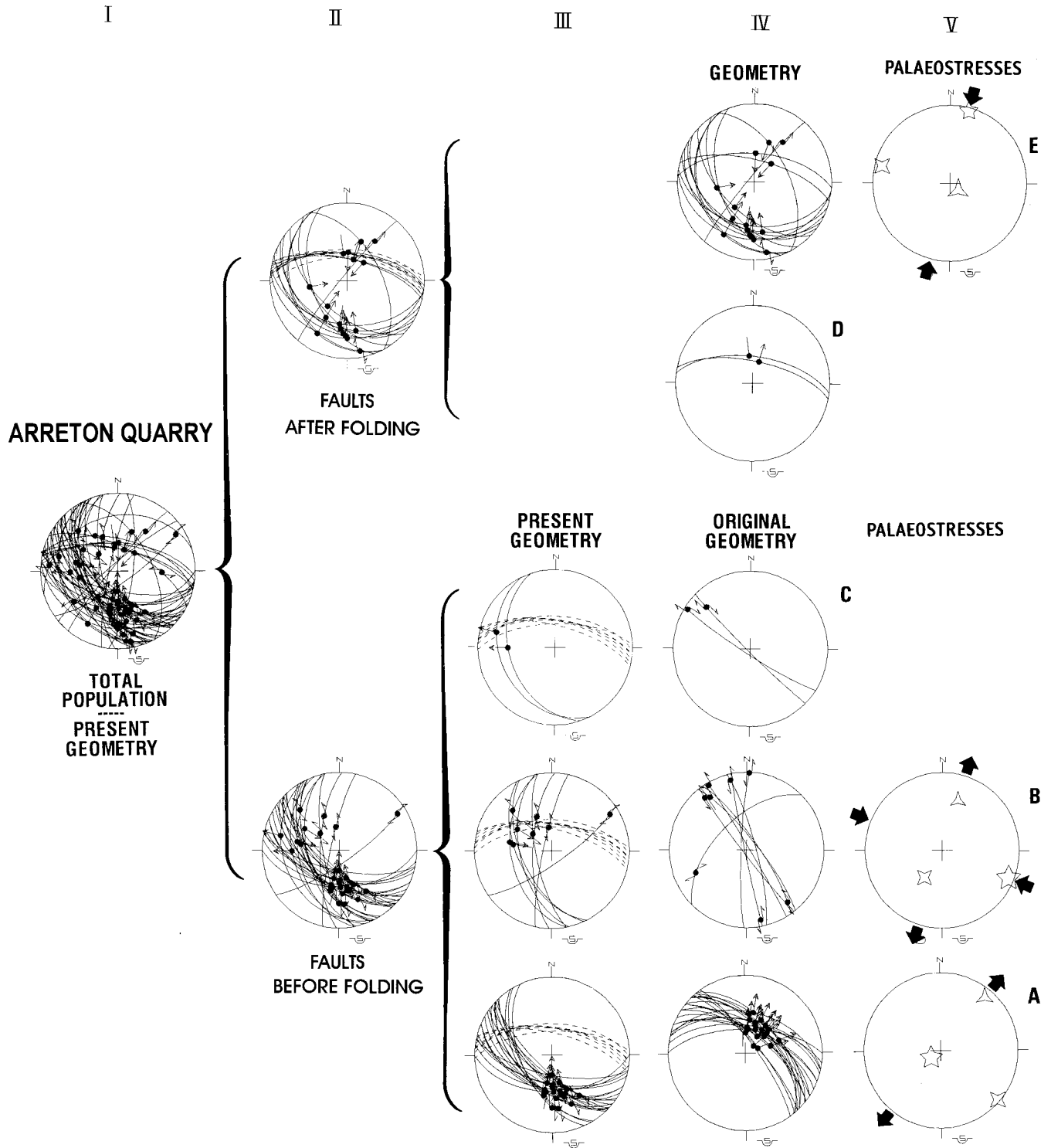


Fig. 7. Geometrical and palaeostress analysis of faulting in Arreton quarry. Explanations and key to stereoplots as for Fig. 6.

(cliffs at Compton Bay) and Fig. 7 (Arreton Quarry). From the total fault population in these two sites (Figs. 6I and 7I), the pre- and post-folding faulting sets have been distinguished on the basis of field evidence of geometrical criteria and chronological relationships between fractures. These two

populations have been separated into different subsets on the basis of relative chronological evidence and mechanical behaviour (Figs. 6II and 7II). For the tensor computation, the faults characterised as pre-tilting (Figs. 6III and 7III) have been back-tilted around the average bedding at each site.

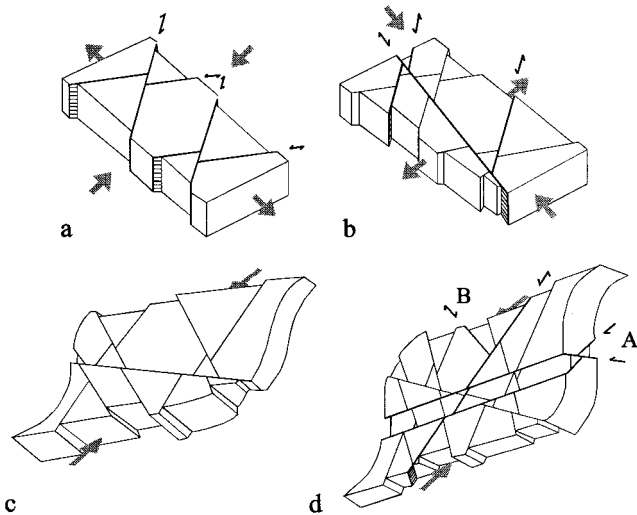


Fig. 8. Polyphase faulting and folding. (a–d) Reconstruction of the four main steps of deformation recognised from the Isle of Wight: (a, b) early conjugate strike-slip faulting prior to folding characterised by ESE–WNW sinistral and ENE–WSW dextral strike-slip faults (a), then ENE–WSW sinistral and NNE–SSW dextral strike-slip faults (b); (c) tilting; (d) late reverse and strike-slip faulting post-folding, characterised respectively by NNE–SSW sinistral and NNW–SSE dextral strike-slip faults (B) and conjugate E–W reverse faults (A). Single and double arrows represent reverse and strike-slip motions, respectively. Large grey arrows illustrate the main direction of compression and extension. The active faults for each step are thick black lines, except for step c (see text for details).

3.3.1. Pre-tilting faulting

Despite their present reverse attitude, the first tectonic event is represented by normal faulting. At the Arreton site, these normal faults are organised in a consistent system with NE–SW extension (Fig. 7IV and VA). At Compton Bay, the faults belonging to this tectonic event are more scattered and less abundant (Fig. 6IVA).

A strike-slip event followed the normal faulting. This second event is characterised by oblique striated faults with a reverse component (Figs. 6III and 7III). After back-tilting, these faults gathered in a conjugate strike-slip system with dextral ENE–WSW and sinistral NW–SE strike-slip faults, corresponding to an ESE–WNW horizontal compression (Figs. 6IV, VB and 7IV, VB).

A second pre-tilting strike-slip system resulted from an NNE–SSW compression (Figs. 6IV, VC and 7IVC). In terms of numbers of faults, this event is less well represented than the previous strike-slip system.

3.3.2. Post-tilting faulting

In the post-tilting fault population, two fault modes have been distinguished: one strike-slip with NE–SW sinistral and NW–SE dextral strike-slip faults, one reverse with ESE–WNW-trending faults. Both systems indicate an N–S compression (Figs. 6IV and 7IV, VE). Some normal faults have also been recognised at the hinge of the flexure (Figs. 6IVD and 7IVD), they are directly related to the flexure process.

More than 80% of the measurement faults have been used

for computations and assigned to one of the above fault systems. The remaining 20% do not fit with these systems and striations on these faults are mostly oblique in their present position and in their tilted position. These faults are interpreted to be related to the stress field that existed during the folding (cf. Bevan, 1984). Their interpretation in terms of stress tensor reconstruction is quite difficult because the angle of tilting at the time of their formation is not known, so it is not possible to put them in their initial position. A rough stress tensor computation shows that they can fit with an N–S compression, thus confirming a continuum in brittle deformation during the inversion process.

The relationships between the successive sets of faults and between faulting and folding (tilting) is summarised schematically in Fig. 8. For each step, the active faults are underlined. Part of the fault population was created during the folding (Bevan, 1984); these syn-folding faults are not underlined on the scheme because they are recognised only locally.

4. Fault slip data sets, palaeostress fields and tectonic events

The different tectonic events characterised in the sites of Compton Bay and Arreton, and described in detail in the previous section, have been recognised at most of the observed sites. The corresponding fault sets and computed stress axes (also see Table 1), for pre-tilting and post-tilting events, are shown in Figs. 9 and 10, respectively.

The complete brittle tectonic analysis allows us to establish the succession of these tectonic events as follows. The first is characterised by generally syn-sedimentary normal faulting in the Upper Chalk and recognised in the Lower and Upper Cretaceous (Fig. 9, Sites 1, 2, 8, 9, 10; Table 1). These normal faults were subsequently tilted and now occur as reverse faults (e.g. Figs. 6 and 7). Generally speaking, this normal fault system is not well developed (Fig. 9) or not easily observed due to the successive later tectonic events that obscure it. Note that, in published seismic data, there is no evidence for syn-sedimentary tectonics in the Upper Chalk (e.g. Butler, 1998; Underhill and Paterson, 1998). Because of the small throws and relative scarcity of the observed faults in the Upper Chalk, we suppose that they represent a transitional stage between the end of the rift-related extensional tectonics and the beginning of the thermal subsidence phase.

The second event is characterised by a system of ENE–WSW to E–W dextral and NNW–SSE sinistral strike-slip faults due to an ESE–WNW compression (Fig. 9, Sites 2, 5, 9, 13, Table 1). This system affects all the Cretaceous Formations and is also tilted. The chronological relationships between this event and the normal faulting are well established, because some of the faults of the previous population of normal faults have been reactivated during this first strike-slip event, as recorded by superimposed striae.

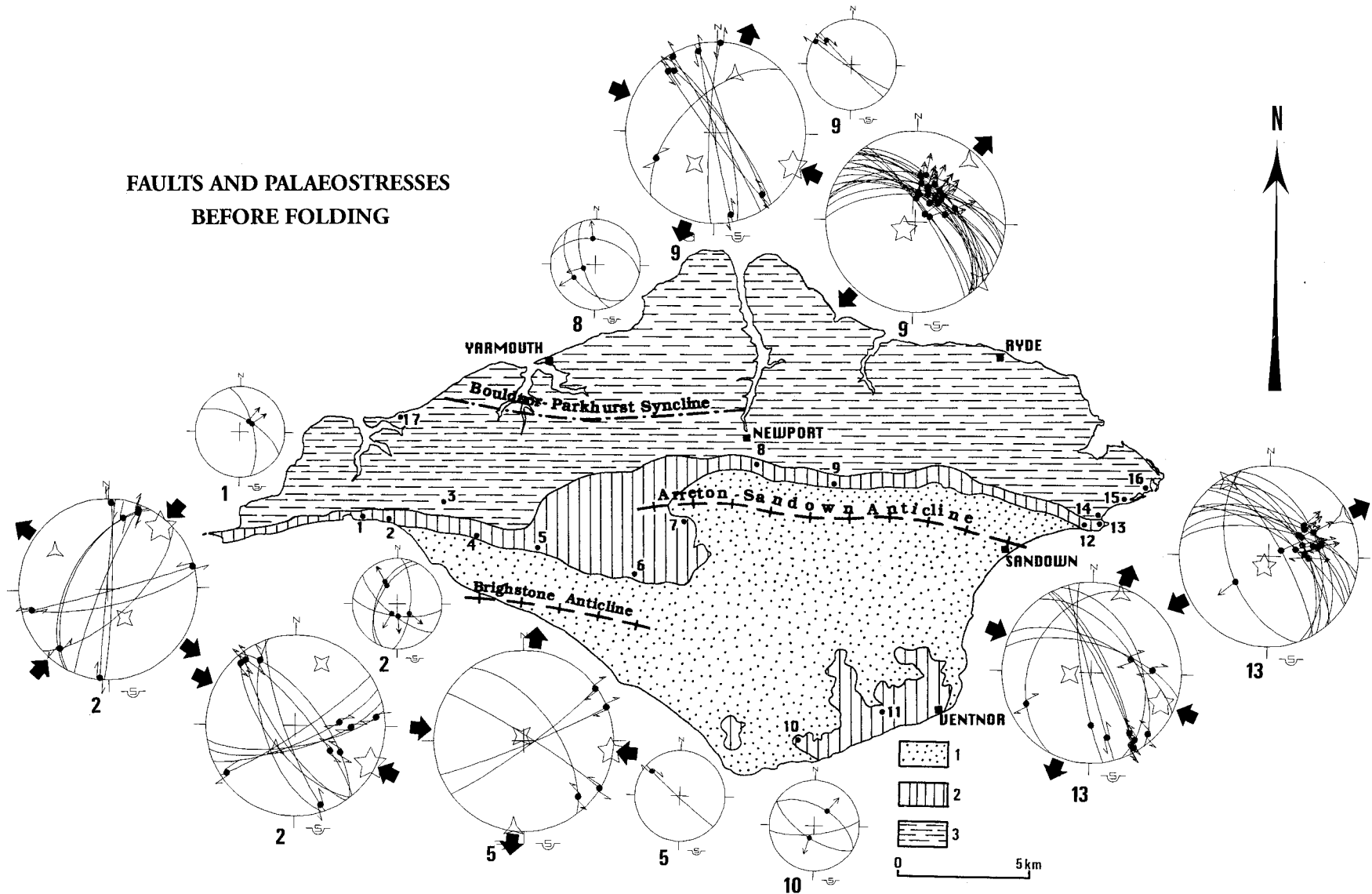


Fig. 9. Geometry and palaeostress tensors of the pre-folding fault population. The large stereoplots represents characteristic examples of syn-sedimentary normal faulting related to NE–SW extension and strike-slip faulting related to ESE–WNW compression, with the corresponding computed stress tensors. Some small stereoplots show the sites where these two events have been recognised, but where the faults were not sufficiently abundant to calculate a reliable stress tensor. All the faults are shown in their original position. Key to stereoplots as for Fig. 6. Key to the map: 1, Lower Cretaceous and part of Upper Cretaceous (Gault Clays to Middle Chalk included); 2, Upper Cretaceous (Upper Chalk); 3, Paleocene–Eocene–Oligocene (Reading Formation to Hamstead Beds included).

**FAULTS AND PALAEOSTRESSES
AFTER FOLDING**

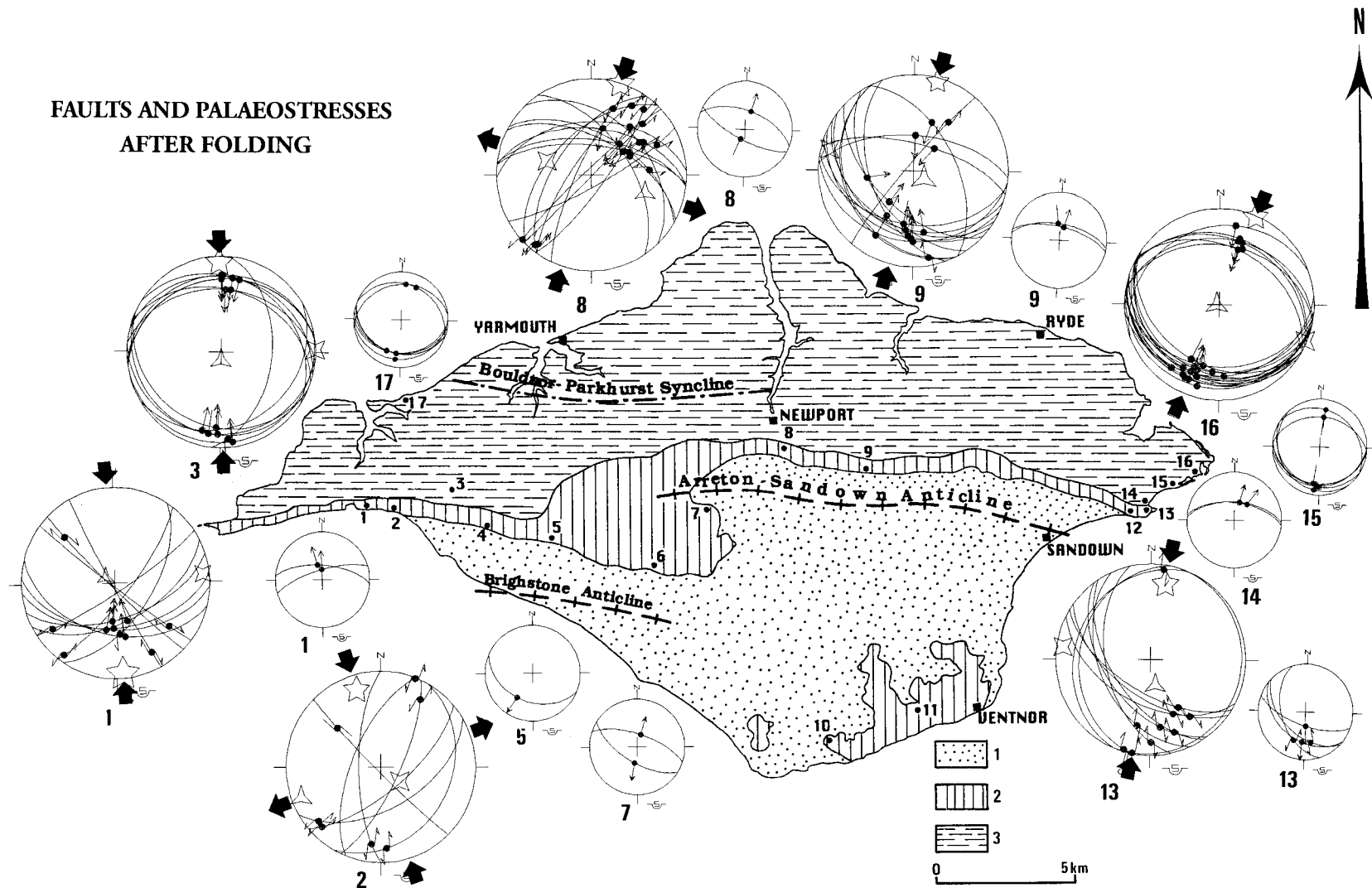


Fig. 10. Geometry and palaeostresses tensors of the post-folding fault population. The large stereoplots represent characteristic examples of reverse and strike-slip faulting, both related to N–S compression, with the corresponding computed stress tensors. Some small stereoplots show the sites where this event has been recognised, but where the faults were not sufficiently abundant to calculate a reliable stress tensor, and some E–W normal faults interpreted as faults developed at the hinge of the flexure axis. Key to stereoplots and map as for Figs. 6 and 9, respectively.

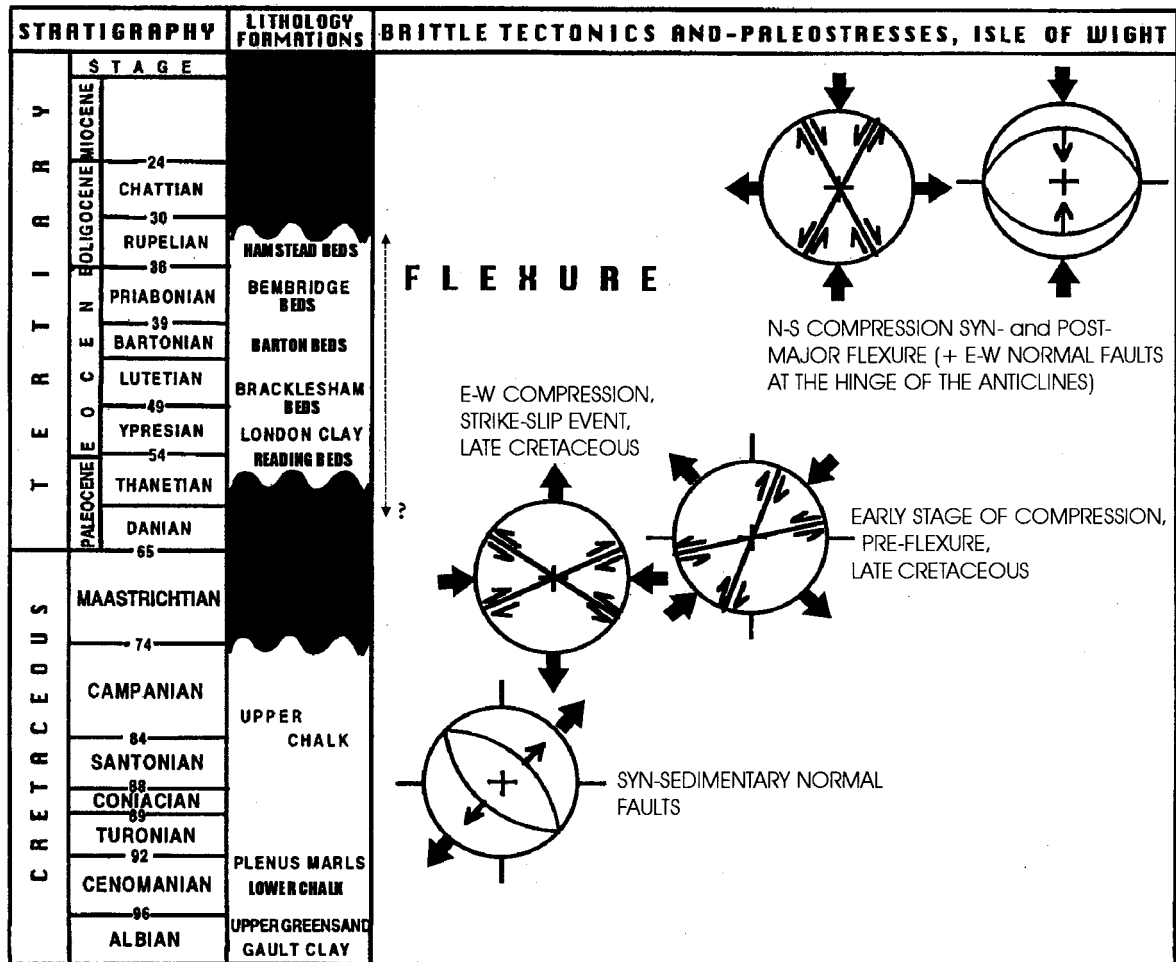


Fig. 11. Brittle tectonics and palaeostress tensors in the Isle of Wight. The diagrams represent schematic fault systems and average stress axes directions for each tectonic event: (1) an early syn-sedimentary Cretaceous extensional regime with normal faulting; (2) two compressional regimes with strike-slip faulting active after Campanian and before Late Paleocene; (3) a N–S compressional event, syn- and post-flexure, expressed by a strike-slip regime and a reverse faulting, associated with E–W normal faulting developed at the hinge of the anticlines, ending after the Priabonian (see text for details).

The third event is characterised by NW–SE to N–S dextral and ENE–WSW sinistral strike-slip faults due to an NE–SW to N–S compression (Fig. 9, Sites 2, 5, 9, Table 1). This event also occurred before folding. It does not affect the Paleocene Formations and is interpreted as an early stage of the compression that will induce the inversion process, which could have occurred during the Maastrichtian–Paleocene gap.

The fourth event post-dates the folding (as demonstrated above, see Section 3.2) and is characterised, on one hand, by E–W to ESE–WNW conjugate reverse faults (Fig. 10, Sites 1, 3, 8, 9, 13, 16, Table 1) and, on the other, by NE–SW sinistral and NW–SE dextral strike-slip faults (Fig. 10, Sites 1, 2, 8, 9, 13, Table 1), both faulting types due to an N–S compression affecting the complete late Mesozoic–Paleocene stratigraphical succession of the Isle of Wight. Some of the reverse faults are inherited and bear two or three generations of slickenside lineations, the reverse related striae being the last ones to develop. A few normal faults (Fig. 10) sometimes accompany the reverse and strike-slip

faulting. Their location is restricted to the apex of the flexure, thereby allowing their interpretation as faults that developed at the hinges of the major anticlines. The N–S shortening related to the flexure process has already been emphasised on the basis of a detailed mesofractures survey by Bevan (1984), who associates later extensional faulting.

The exact inversion age in the Isle of Wight–Purbeck area remains uncertain, ranging from the end of Eocene to Miocene, according to different authors (e.g. Butler, 1998; Butler and Pullan, 1990; Chadwick, 1993; Gale et al., 1999). However, given that all the outcropping formations are affected by this last faulting episode, we suggest that the latest expression of inversion on the Isle of Wight is at least Oligocene.

5. Conclusions

Application of inversion methods to brittle deformation (Angelier, 1984) permits the mechanical characterisation of

Late Cretaceous and Cenozoic deformation in the Isle of Wight. The evolution of brittle tectonic deformation and related palaeostresses during the Upper Cretaceous and Paleogene, in the framework of the Wessex Basin Extension and of the Purbeck–Isle of Wight monocline development, is summarised in Fig. 11. Despite important later compressive deformations, some traces of syn-sedimentary extensional tectonics are recognised in the Upper Chalk in several sites on the Isle of Wight. This is followed by an E–W to ESE–WNW compression marked by strike-slip meso-faulting, but no major tectonic features. This compression would correspond to the tectonic expressions identified by some authors on the basis of sedimentary structures during the Late Cretaceous. Subsequently, the major inversion phase is characterised, in terms of brittle deformation, by three stages of faulting. The first stage is strike-slip in type, pre-flexure and recognisable in a few sites, and related to a roughly NNE–SSW compression. The second stage of faulting is directly related to the flexure process within an N–S compressive regime. The third stage is post-flexure and is characterised by well-developed systems of strike-slip and reverse faults related to the end of the N–S compressive period. This stage 3 faulting demonstrates that the compressive regime still existed after the main folding process, at least until the beginning of the Oligocene.

These results highlight the relationships between the faulting and folding since the end of the extensional process to the end of the inversion process and constrain the different states of deformation. Some evidence of syn-sedimentary normal faulting has been detected in the Upper Chalk, demonstrating the persistence of minor extension during thermal subsidence. Finally, the inversion tectonics are marked not only by a folding process, but also by further increments of faulting: strike-slip faults developed prior to, during and after the flexure process, accompanied in the post-flexure stage by development of reverse faults.

Acknowledgements

Financial support for this work was provided by the Belgian–French Scientific Cooperation (MAE-CGRI) and by the British–French collaboration program “Alliance”. Special thanks are given to Dr. Christian Dupuis, who participated in the early stages of the field work, for helpful information and discussions. We acknowledge Dr. J. Turner, Dr. T.G. Bevan and Dr. J.R. Underhill for their advice and constructive reviews and for improving the English of this paper. S.V. is a research associate at the National Research Foundation of Belgium.

References

- Ainsworth, N.R., Braham, W., Gregory, F.J., Johnson, B., King, C., 1998a. A proposed latest Triassic to earliest Cretaceous microfossil biozonation for the English Channel and its adjacent areas. In: Underhill, J.R. (Ed.), *Development, Evolution and Petroleum Geology of the Wessex Basin*. Geological Society Special Publication 133, pp. 87–102.
- Ainsworth, N.R., Braham, W., Gregory, F.J., Johnson, B., King, C., 1998b. The lithostratigraphy of the latest Triassic to earliest Cretaceous of the English Channel and its adjacent areas. In: Underhill, J.R. (Ed.), *Development, Evolution and Petroleum Geology of the Wessex Basin*. Geological Society Special Publication 133, pp. 103–164.
- Ameen, M.S., 1990. Macrofaulting in the Purbeck–Isle of Wight monocline. *Proceedings of the Geologists Association* 101, 31–46.
- Anderson, E.M., 1942. *The dynamics of faulting*. Oliver & Boyd, Edinburgh.
- Angelier, J., 1984. Tectonic analysis of fault slip data sets. *Journal of Geophysical Research* 89 (B7), 5835–5848.
- Angelier, J., 1990. Inversion of field data in fault tectonics to obtain the regional stress—III. A new rapid direct inversion method by analytical means. *Geophysics Journal International* 103, 363–376.
- Angelier, J., 1994. Fault slip analysis and palaeostress reconstruction. In: Hancock, P.L. (Ed.), *Continental Deformation*. Pergamon Press, Oxford, pp. 53–100.
- Angelier, J., Barrier, E., Chu, H.T., 1986. Plate collision and paleostress trajectories in a fold-thrust belt: the foothills of Taiwan. *Tectonophysics* 125, 161–178.
- Bergerat, F., 1985. *Déformations cassantes et champ de contraintes tertiaires dans la plate-forme européenne*. Ph.D. thesis, University Paris VI.
- Bergerat, F., 1987. Stress fields in the European platform at the time of Africa–Eurasia collision. *Tectonics* 6 (2), 99–132.
- Bergerat, F., Vandycke, S., 1994. Cretaceous and Tertiary fault systems in the Boulonnais and Kent areas: paleostress analysis and geodynamical implications. *Journal of the Geological Society of London* 151, 439–448.
- Bevan, T.G., 1984. Tectonic evolution of the Isle of Wight: a Cenozoic stress history based on mesofractures. *Proceedings of the Geologists Association* 96, 227–235.
- Bevan, T.G., 1985. A reinterpretation of fault systems in the Upper Cretaceous rocks of the Dorset coast, England. *Proceedings of the Geologists Association* 96, 337–342.
- Bevan, T.G., Hancock, P.L., 1986. A late Cenozoic regional mesofracture system in southern England and northern France. *Journal of the Geological Society of London* 143, 355–362.
- Bouroz, C., Angelier, J., Bergerat, F., 1989. De la distribution des diaclases dans des flexures à la chronologie tectonique: exemples dans le Plateau du Colorado (Utah–Arizona–Nouveau Mexique, USA). *Geodinamica Acta* 3 (4), 305–318.
- Butler, M., 1998. The geological history of the southern Wessex Basin—a review of new information from oil exploration. In: Underhill, J.R. (Ed.), *Development, Evolution and Petroleum Geology of the Wessex Basin*. Geological Society Special Publication 133, pp. 67–86.
- Butler, M., Pullan, C.P., 1990. Tertiary structures and hydrocarbon entrapment in the Weald Basin of Southern England. In: Hardman, R.F.P., Brooks, J. (Eds.), *Tectonic Events Responsible for Britain’s Oil and Gas Reserves*. Geological Society Special Publication 55, pp. 371–391.
- Chadwick, R.A., 1993. Aspects of basin inversion in southern Britain. *Journal of the Geological Society* 150, 311–322.
- Cole, D.C., Harding, I.C., 1998. Use of palynofacies analysis to define Lower Jurassic (Sinemurian to Pliensbachian) genetic stratigraphic sequences in the Wessex Basin, England. In: Underhill, J.R. (Ed.), *Development, Evolution and Petroleum Geology of the Wessex Basin*. Geological Society Special Publication 133, pp. 165–185.
- Coulon, M., 1992. La distension oligocène dans le nord-est du Bassin de Paris (perturbation des directions d’extension et distribution des stylonites). *Bulletin de la Société Géologique de France* 163 (5), 531–540.
- Gale, A.S., Jeffery, P.A., Huggett, J.M., Connolly, P., 1999. Eocene inversion of the Sandown Pericline, Isle of Wight, southern England. *Journal of the Geological Society* 156, 327–339.
- Hamblin, R.J.O., Crosby, A., Balson, P.S., Jones, S.M., Chadwick, R.A.,

- Penn, I.E., Arthur, M.J., 1992. United Kingdom Offshore Regional Report: the Geology of the English Channel. HMSO, London.
- Hancock, P.L., 1985. Brittle microtectonics: principle and practice. *Journal of Structural Geology* 7, 437–457.
- Hawkes, P.W., Fraser, A.J., Einchcomb, C.C.G., 1998. The tectono-stratigraphic development and exploration history of the Weald and Wessex Basins, Southern England, U.K.. In: Underhill, J.R. (Ed.), *Development, Evolution and Petroleum Geology of the Wessex Basin*. Geological Society Special Publication 133, pp. 39–65.
- Jenkyns, H.C., Senior, J.R., 1991. Geological evidence for intra-Jurassic faulting in the Wessex Basin and its margins. *Journal of the Geological Society* 148, 245–260.
- Kent, P.E., 1949. A structure–contour map of the surface of the buried pre-Permian rocks in England and Wales. *Proceedings of the Geologists Association* 60, 87–104.
- Lake, S.D., Karner, G.D., 1987. The structure and evolution of the Wessex Basin, southern England: an example of inversion tectonics. *Tectonophysics* 137, 347–378.
- Nowell, D.A.G., 1995. Faults in the Purbeck–Isle of Wight monocline. *Proceedings of the Geologists Association* 106, 145–150.
- Reches, Z., 1978. Development of monoclines, part I. Structure of the Palisades Creek branch of the East Kaibab monocline, Grand Canyon, Arizona, Laramide folding associated with basement block faulting in the western United States. In: Matthews, V. (Ed.), *Memoir of the Geological Society of America* 151, pp. 235–271.
- Reches, Z., Johnson, A.M., 1978. Development of monoclines, part II. Theoretical analysis of monoclines. In: Matthews, V. (Ed.), *Memoir of the Geological Society of America* 151, pp. 273–311.
- Stoneley, R., 1982. The structural development of the Wessex basin. *Journal of the Geological Society* 139, 545–552.
- Turner, J.P., Hancock, P.L., 1990. Relationships between thrusting and joint systems in the Jaca thrust-top basin, Spanish Pyrenees. *Journal of Structural Geology* 12, 217–226.
- Underhill, J.R., Paterson, S., 1998. Genesis of tectonic inversion structures: seismic evidence for the development of key structures along the Purbeck–Isle of Wight Disturbance. *Journal of the Geological Society* 155, 975–992.
- Underhill, J.R., Stoneley, R., 1998. Introduction to the development, evolution and petroleum geology of the Wessex basin. In: Underhill, J.R. (Ed.), *Development, Evolution and Petroleum Geology of the Wessex Basin*. Geological Society Special Publications 133, pp. 1–18.
- Vandycke, S., Bergerat, F., 1989. Analyse microtectonique des déformations cassantes dans le Bassin de Mons. Reconstitution des paléochamps de contrainte au Crétacé–Tertiaire. *Annales Société Géologique de Belgique* 112 (2), 479–487.
- Vandycke, S., Bergerat, F., 1992. Tectonique de failles et paléocontraintes dans les formations crétacées du Boulonnais (N. France). *Bulletin Société Géologique de France* 163 (5), 553–560.
- Vandycke, S., Bergerat, F., Dupuis, C., 1991. Meso-Cenozoic faulting and inferred paleostresses of the Mons basin (Belgium). *Tectonophysics* 192, 261–271.